Journal of Medicinal Chemistry Article

J. Med. Chem. **2009,** *52,* 5429–5441 **5429**
DOI: 10.1021/jm900627v

Benzothiopyranoindole-Based Antiproliferative Agents: Synthesis, Cytotoxicity, Nucleic Acids Interaction, and Topoisomerases Inhibition Properties

Lisa Dalla Via,*[,†] Sebastiano Marciani Magno,[†] Ornella Gia,[†] Anna Maria Marini,*[,‡] Federico Da Settimo,[‡] Silvia Salerno,[‡] Concettina La Motta,[‡] Francesca Simorini,[‡] Sabrina Taliani,[‡] Antonio Lavecchia,[§] Carmen Di Giovanni,[§] Giuseppe Brancato,[§] Vincenzo Barone,[∥] and Ettore Novellino[§]

[†]*Dipartimento di Scienze Farmaceutiche, Università di Padova, via Marzolo 5, I-35131 Padova, Italy,* [‡]*Dipartimento di Scienze Farmaceutiche, Università di Pisa, via Bonanno 6, I-56126 Pisa, Italy,* [§]*Dipartimento di Chimica Farmaceutica e Tossicologica, Università di Napoli Federico II, Via D. Montesano 40, I-80131 Napoli, Italy, and* [∥]*Scuola Normale Superiore, Piazza dei Cavalieri 7, I-56100, Pisa and Istituto per i Processi Chimico-Fisici del Consiglio Nazionale delle Ricerche (IPCF-CNR), Area della Ricerca, Via G. Moruzzi 1, I-56124 Pisa, Italy*

Received May 12, 2009

Novel benzo[3′,2′:5,6]thiopyrano[3,2-*b*]indol-10(11*H*)-ones **1a**−**v** were synthesized and evaluated for their antiproliferative activity in an in vitro assay of human tumor cell lines (HL-60 and HeLa). Compounds **1e**−**v**, substituted at the 11-position with a basic side chain, showed a significant ability to inhibit cell growth with IC_{50} values in the low micromolar range. Linear dichroism measurements showed that all 11-dialkylaminoalkyl substituted derivatives **1e**−**v** behave as DNA-intercalating agents. Fluorimetric titrations demonstrated their specificity in binding to A−T rich regions, and molecular modeling studies were performed on the most active derivatives (**1e**, **1i**, **1p**) to characterize in detail the complexation mechanism of these benzothiopyranoindoles to DNA. A relaxation assay evidenced a dose-dependent inhibition of topoisomerase II activity that appeared in accordance with the antiproliferative capacity. Finally, for the most cytotoxic derivative, **1e**, a topoisomerase II poisoning effect was also demonstrated, along with a weak inhibition of topoisomerase I-mediated relaxation.

Downloaded by TATA INST OF FUNDAMENTAL RES on October 11, 2009 | http://pubs.acs.org
Publication Date (Web): August 19, 2009 | doi: 10.1021/jm900627v

Introduction

The incidence of cancer, the main cause of mortality after cardiovascular diseases, has significantly increased in the past few years; therefore, an important goal of today's research is the development of new drugs characterized by promising antiproliferative properties, in particular against the most aggressive tumors.[1−4] Anticancer agents that target DNA are among the most effective and have produced significant increases in the survival rates of patients, especially when used in combination protocols with drugs that have different mechanisms of action.[5,6] Among chemotherapeutic drugs, DNA-intercalating agents, such as anthracyclines, *m*-amsacrine (*m*-AMSA[a]), or ellipticines, represent a peculiar group with excellent antitumor activity.[7,8] The intercalators give rise to an effective nuclear DNA binding complex, affording a distorted helix and affecting the activity of processing enzymes, thus compromising the structure and physiological functions of the macromolecule.[9,10] More interestingly, several DNA-intercalating agents are able to affect topoisomerases I and/or II catalytic activity by forming a stable ternary complex involving the drug, the enzyme, and DNA and producing permanent DNA strand breaks.[11−14]

In actively replicating cells, topoisomerases I and II are involved in many aspects of DNA metabolism and chromatin topology. The enzymes relieve torsional stresses caused during DNA replication and transcription, cutting and rejoining of single, topoisomerase I, or double, topoisomerase II, DNA strands.[15−19] Topoisomerase-targeting agents have long been considered an attractive target for the design of cancer chemotherapeutics because they can cause permanent DNA damage that triggers a series of cellular events, inducing apoptosis and finally causing cell death.[20−26] However, despite their antitumor potency, several drugs that act as intercalators and topoisomerase targeting agents suffer from poor solubility, dose-limiting toxicity, reversibility of cleavage-complex formation, and resistance mechanism development;[27−29] for these reasons, novel molecules are being developed to overcome such limitations.[30−33] From a structural point of view, DNA-intercalating ligands are characterized by a planar (hetero)-aromatic polycyclic moiety, a common pharmacophoric feature, and are able to form molecular complexes between DNA base pairs, which are stabilized via hydrophobic interactions, hydrogen bonding, and/or van der Waal's forces. Moreover, in spite of the undoubted importance of the planar chromophore, the presence of charged groups or of protonable nitrogen atom-bearing side chains in an appropriate position on the planar core improves the binding affinity, allowing further interactions of the ligands with other important architectural features of DNA such as its major or minor grooves. Finally, an enhanced solubility under physiological conditions can be envisaged.[34−36]

As part of our research program devoted to the preparation and evaluation of new antiproliferative agents, we extensively studied several polycyclic chromophores that are structurally

*To whom correspondence should be addressed. Phone: +39 049 8275712. Fax: +39 049 8275366. E-mail: lisa.dallavia@unipd.it.

[a] Abbreviations: *m*-AMSA, *m*-amsacrine (4′-(9-acridinylamino)methanesulfon-*m*-anisidide); LD, linear flow dichroism; DFT, density functional theory; PCM, polarizable continuum model; SDS, sodium dodecyl sulfate; BSA, bovine serum albumin.

© 2009 American Chemical Society

Published on Web 08/19/2009

Chart 1. Structures of Compounds **I**−**VI**

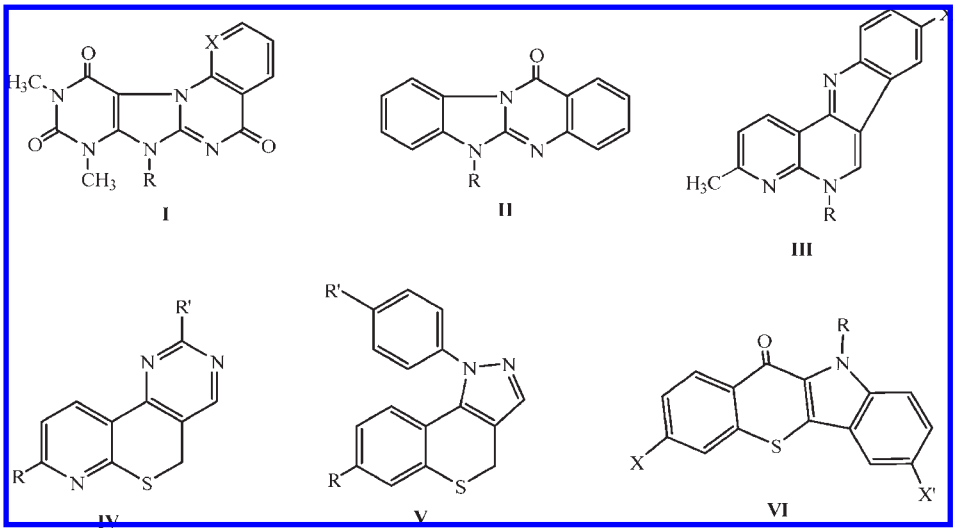

Downloaded by TATA INST OF FUNDAMENTAL RES on October 11, 2009 | http://pubs.acs.org
Publication Date (Web): August 19, 2009 | doi: 10.1021/jm900627v

correlated to classes of DNA-intercalating agents, among which we discovered new compounds (Chart 1) incorporating the purine (**I**), benzimidazole (**II**), and indole (**III**) moieties that are endowed with a significant cytotoxic activity, which is comparable to that of ellipticine. These compounds exhibited the ability to intercalate with DNA and in some cases to inhibit topoisomerase II, properties which were found to be affected by the presence, the nature, or the spatial orientation of the pendant side alkyl chains.[37−39] We then extended our interest to the design and synthesis of new heterocycles, obtained by using as "synthetic tools" the pyridothiopyrane and the benzothiopyrane moieties, which demonstrated to be versatile intermediates. Several compounds (**IV** and **V**, Chart 1) evaluated on human tumor cell lines showed a detectable cytotoxic activity, thus appearing to be interesting chromophore systems.[40,41]

These results prompted us to synthesize a series of the new tetracyclic benzothiopyranoindoles of the general formula **VI** (Chart 1), bearing a methoxy group or a chlorine in either the 3 or the 7 position of the planar moiety; furthermore, the NH group (position 11) of the indole moiety allowed us the possibility to insert suitable pendant protonable dialkylaminoalkyl side chains.

The ability of the new benzothiopyranoindole derivatives to exert an antiproliferative activity was evaluated by means of an inhibition growth assay on two human tumor cell lines, human promyelocitic leukemic (HL-60) and human cervix adenocarcinoma (HeLa) cells. Linear flow dichroism (LD) experiments were performed to assess the occurrence of a molecular complex with DNA. Then the thermodynamic parameters for the binding process were calculated by fluorimetric titration. To further understand the binding mode of these molecules to DNA at the atomic level, a molecular modeling study was carried out using both flexible docking and ab initio quantum mechanical calculations as suggested by the biophysical measurements. Finally, the ability of the compounds to interfere with the activity of both topoisomerases I and II was also evaluated.

Chemistry

The preparation of the 7- and/or 3-substituted benzo[3′,2′:5,6]thiopyrano[3,2-*b*]indol-10(11*H*)-ones **1a**−**d** and of the 11-dialkylaminoalkyl substituted derivatives **1e**−**v** was performed following the synthetic procedure described in Scheme 1. The preparation of the key starting 7-methoxy- and 7-chloro-3-hydroxymethylenebenzothiopyranone derivatives **2a**−**b** was accomplished from the suitable 7-methoxy- or 7-chloro-2,3-dihydrobenzo[3′,2′:5,6]thiopyran-4(4*H*)-one, following previously described procedures.[41] Compounds **2a**−**b**, containing a methine active group, gave the desired 3-phenylhydrazono intermediates **3a**−**d**, in particularly good yields, by coupling with the appropriately *p*-substituted diazonium salt using the Japp−Klingemann reaction.[42] Compounds **3a**−**d** were directly converted to the desired indoles **1a**−**d** using the Fischer cyclization, by refluxing in ethanolic hydrogen chloride solution, with good to high yields. All the structures proposed for the final compounds agreed with IR and ^{1}H NMR spectral data, in which an interesting feature was the low field signal ($\delta \approx 12$ ppm), which was exchangeable with D_2O and was assigned to the proton of the indole NH group.

The target 11-*N*-dialkylaminoalkyl substituted derivatives **1e**−**v** were obtained by reaction of compounds **1a**−**d** with the appropriate dialkylaminoalkyliodide hydroiodides in anhydrous DMF solution in the presence of sodium hydride. Dialkylaminoalkyliodide hydroiodides were prepared from the corresponding commercially available dialkylaminoalkylchloride hydrochorides,[43] as the latter gave only poor yields in the alkylation reactions. IR and ^{1}H NMR spectral data of compounds **1e**−**v** were consistent with the proposed structure. Finally, for the biological assays, compounds **1e**−**v** were transformed into their hydrochlorides by treatment with hydrogen chloride-saturated ethanol solution.

Results and Discussion

Antiproliferative Activity. The ability of new derivatives to inhibit cell growth was evaluated by means of an in vitro assay performed on two human tumor cell lines, HeLa (cervix adenocarcinoma) and HL-60 (promyelocytic leukemia). The results, expressed as IC_{50} values, i.e., the concentration (μM) of compound able to produce 50% cell death with respect to the control culture, are shown in Table 1. Ellipticine was used as a reference compound.[39]

The results obtained demonstrate that the unsubstituted tetracyclic chromophore (**1a**−**d**), independent of the group X

Scheme 1. Preparation of 3,7-Substituted-11-dialkylaminoalkyl-benzo[3′,2′:5,6]thiopyrano[3,2-*b*]indol-10(11*H*)-ones **1a**−**v**[a]

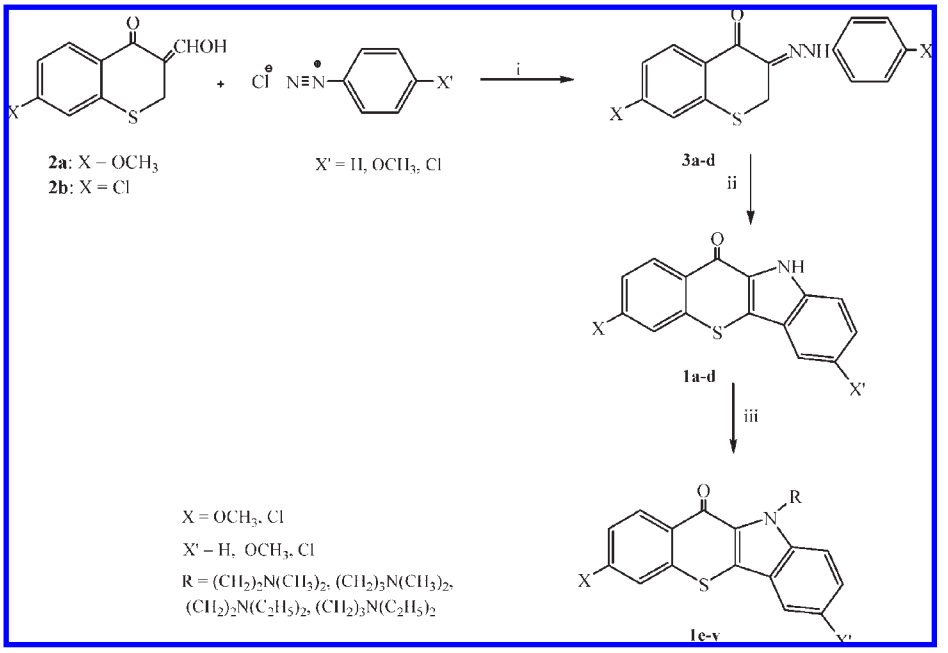

[a] Reagents and conditions: (i) AcONa, MeOH; (ii) EtOH HCl, Δ; (iii) RI HI, NaH, DMF,Δ.

Table 1. Chemical Structure and Cell Growth Inhibition in the Presence of Examined Compounds

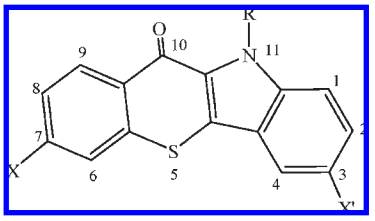

				cell lines IC_{50} (μM)	
compd	X	X′	R	HL-60	HeLa
1a	OCH_3	H	H	> 20	> 20
1b	OCH_3	OCH_3	H	> 20	> 20
1c	OCH_3	Cl	H	> 20	> 20
1d	Cl	H	H	> 20	> 20
1e	OCH_3	H	$(CH_2)_2N(CH_3)_2$	0.41 ± 0.08	1.30 ± 0.10
1f	OCH_3	H	$(CH_2)_2N(C_2H_5)_2$	1.80 ± 0.06	2.70 ± 0.05
1g	OCH_3	H	$(CH_2)_3N(CH_3)_2$	1.90 ± 0.08	2.90 ± 0.3
1h	OCH_3	H	$(CH_2)_3N(C_2H_5)_2$	2.40 ± 0.08	3.90 ± 0.6
1i	OCH_3	OCH_3	$(CH_2)_2N(CH_3)_2$	0.66 ± 0.17	2.15 ± 0.50
1l	OCH_3	OCH_3	$(CH_2)_2N(C_2H_5)_2$	1.10 ± 0.06	2.30 ± 0.40
1m	OCH_3	OCH_3	$(CH_2)_3N(CH_3)_2$	1.35 ± 0.10	2.60 ± 0.30
1n	OCH_3	OCH_3	$(CH_2)_3N(C_2H_5)_2$	1.50 ± 0.12	2.50 ± 0.30
1o	OCH_3	Cl	$(CH_2)_2N(CH_3)_2$	1.17 ± 0.12	1.82 ± 0.87
1p	OCH_3	Cl	$(CH_2)_2N(C_2H_5)_2$	0.71 ± 0.09	1.12 ± 0.20
1q	OCH_3	Cl	$(CH_2)_3N(CH_3)_2$	1.07 ± 0.24	1.85 ± 0.21
1r	OCH_3	Cl	$(CH_2)_3N(C_2H_5)_2$	1.02 ± 0.18	1.68 ± 0.25
1s	Cl	H	$(CH_2)_2N(CH_3)_2$	1.31 ± 0.17	1.53 ± 0.24
1t	Cl	H	$(CH_2)_2N(C_2H_5)_2$	3.21 ± 0.39	4.33 ± 0.80
1u	Cl	H	$(CH_2)_3N(CH_3)_2$	7.19 ± 0.69	14.05 ± 1.76
1v	Cl	H	$(CH_2)_3N(C_2H_5)_2$	2.64 ± 0.60	2.91 ± 0.11
ellipticine[a]				0.66 ± 0.02	0.29 ± 0.01

[a] Taken from ref 39.

or X′ inserted in the 7 and/or 3 positions, is ineffective in inducing cell death.

The ability of the derivatives characterized by the insertion of an alkylaminoalkyl side chain (**1e**−**v**) to exert a significant antiproliferative effect on both cell lines is demonstrated by IC_{50} values ranging from 0.41 to 14.05 μM, thus suggesting the important role played by the protonable dialkylamino side chains; moreover, the HL-60 cells are more sensitive to the effect exerted by all the active compounds than HeLa cells. Furthermore, comparing the antiproliferative effect exerted by analogous compounds having the same substituents X and X′ on the tetracyclic nucleus, but carrying different dialkylaminoalkyl side chains, it can be affirmed that within the subseries characterized by a methoxy group or a chlorine in the 7 (X) and a hydrogen or a methoxy in the 3 (X′) position, the insertion of the dimethylaminoethyl chain confers the higher cytotoxic ability (compounds **1e**, **1i**, and **1s**). In particular, compound **1e**, characterized by a methoxy group and a hydrogen in positions 7 and 3, respectively, is the most active on HL-60 cells, showing an IC_{50} value lower than that of ellipticine; a notable antiproliferative ability, comparable to that of the reference compound, is also shown by the 3,7-dimethoxy substituted compound **1i**. On the other hand, the derivatives carrying the dimethylaminopropyl or diethylaminoalkyl side chains, show, within each class of analogues, a lower cytotoxic capacity, thus indicating that an increase in length and steric hindrance of the side chain seems to be detrimental on the antiproliferative activity.

Derivatives **1o**−**r** bearing a chlorine in the 3- position and a 7-methoxy group, displayed similar cytotoxic potencies, ranging from 0.71 μM (**1p**) to 1.17 μM (**1o**), indicating that in this group of analogues the dependence of cellular effects on the type of the basic chain appears less emphasized. Thus, to exert a significant antiproliferative effect, the benzothiopyranoindole moiety requires the presence of a basic side chain, preferably the dimethylaminoethyl one, at the 11-position of the heterocyclic scaffold.

Downloaded by TATA INST OF FUNDAMENTAL RES on October 11, 2009 | http://pubs.acs.org
Publication Date (Web): August 19, 2009 | doi: 10.1021/jm900627v

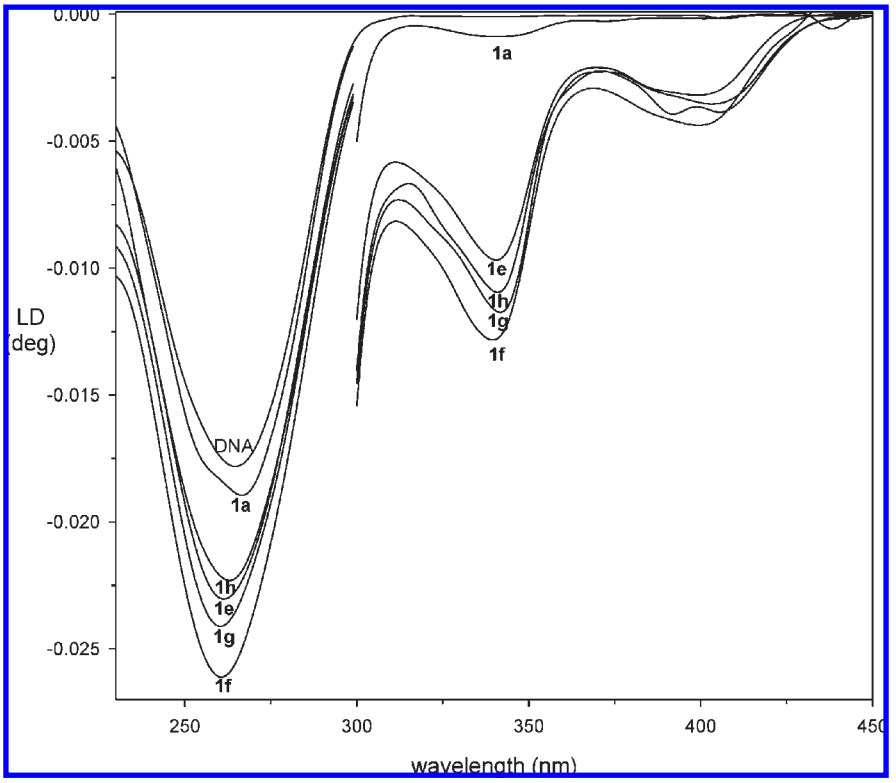

Figure 1. LD spectra for compounds **1a** and **1e**−**h** at [drug]/[DNA] = 0.04. [DNA] = 1.9×10^{-3} M. Four other experiments gave similar results.

Interaction with DNA. The study of the mechanism of action responsible for the antiproliferative activity of the new derivatives prompted us to investigate on the ability of the heterocyclic nucleus to form a molecular complex with DNA. To pursue this question, LD experiments were performed in the presence of salmon testes DNA at different [drug]/[DNA] ratios. The spectra of DNA solutions in the presence of the structurally related compounds **1a** and **1e**−**h** are reported in Figure 1. The DNA spectrum presents the typical negative dichroic signal at 260 nm, while in the presence of new benzothiopyranoindoles, a further negative signal at higher wavelength occurs. Nevertheless, the intensity of this signal is significantly reduced for **1a**, which is characterized by the absence of the protonable side chain. The same behavior was also observed for the other compounds, i.e., a small negative induced signal for the unsubstituted benzothiopyranoindoles (**1b**−**d**) and a large significant signal for the corresponding derivatives carrying the dialkylaminoalkyl side chains (**1i**−**v**) (spectra not shown). These results suggest that the tetracyclic chromophore may insert between base pairs and that this capacity becomes significantly more pronounced if a dialkylaminoalkyl chain is inserted. It is reasonable that the presence of a basic nitrogen, protonable at physiological pH, facilitates the interaction between the nucleic acid and the charged compound, thus making the intercalative process more effective.

Binding Studies. To investigate the interaction of the new benzothiopyranoindoles with nucleic acid base pairs more in depth, fluorimetric titrations in the presence of DNA characterized by a different base composition and of synthetic polyDNAs, poly[dA-dT]poly[dA-dT], and poly[dG-dC]poly[dG-dC] were performed. On the basis of preliminary data, the fluorimetric determinations were carried out with derivative **1i**, one of the most active in inducing the antiproliferative effect, and characterized by a constant intensity in fluorescence emission throughout the duration of the experiment. Figure 2A shows that the different aliquots of **1i** that lead to the concentration [*B*], in mmol of **1i** per mol of nucleic acid, of a complex with the double helix, plotted versus the free quantity [*F*], in mmol of **1i** per mol of nucleic acid, tend to saturation. Moreover, the binding data were plotted as a dependence of [*B*]/[*F*] on [*B*], thus in the Scatchard data representation framework, and analyzed by a general thermodynamic model described elsewhere (Figure 2B).[44a,44b] The simulated curves (lines) that satisfactorily fitted the experimental data (symbols) are typical for two binding sites, named S_1 and S_2, both with monocoordination.[44a,44b] The obtained binding results are summarized in Table 2. The total binding site concentration (B_{max}) varies significantly between the different nucleic acids and, interestingly, points out a certain preference of the benzothiopyranoindole ligand for the thymine−adenine base pair.

Moreover, the **1i** distribution between S_1 and S_2 sites is very different. Indeed, the maximum binding concentration of **1i** on the S_1 site, B_{max1}, is notably lower with respect to that of the S_2 site, B_{max2}, and does not show any significant variation depending on the base pair composition. In contrast, B_{max2} varies according to base composition, in agreement with the behavior evidenced for B_{max}. These differences in binding capacity of **1i** between S_1 and S_2, suggest different roles for them and the contribution of two binding events to the overall binding process. Furthermore, taking into consideration that **1i** is characterized by two main structural motifs, consisting in a heteropolycyclic nucleus and a basic side chain, it could be hypothesized that the interaction between **1i** and the nucleic acid occurs owing to two distinct processes. The first consists in electrostatic interactions that

Downloaded by TATA INST OF FUNDAMENTAL RES on October 11, 2009 | http://pubs.acs.org
Publication Date (Web): August 19, 2009 | doi: 10.1021/jm900627v

take place between the side chain of **1i** and the polyanion skeleton of the nucleic acid, and the second process deals with an intercalative complexation, mediated by weak interactions. In more detail, the dependence of B_{max2} on base composition suggests the participation of this site at the intercalative event, while the independence of B_{max1} could indicate that S_1 is the site involved in the ion pair interactions. The calculated values for the association constants, k_1 and k_2, corresponding to S_1 and S_2 sites, respectively, reinforced this assumption. Indeed, the significantly higher values of k_1 with respect to k_2 could reflect the involvement of strong and weak binding forces for the binding to S_1 and S_2 sites, respectively.

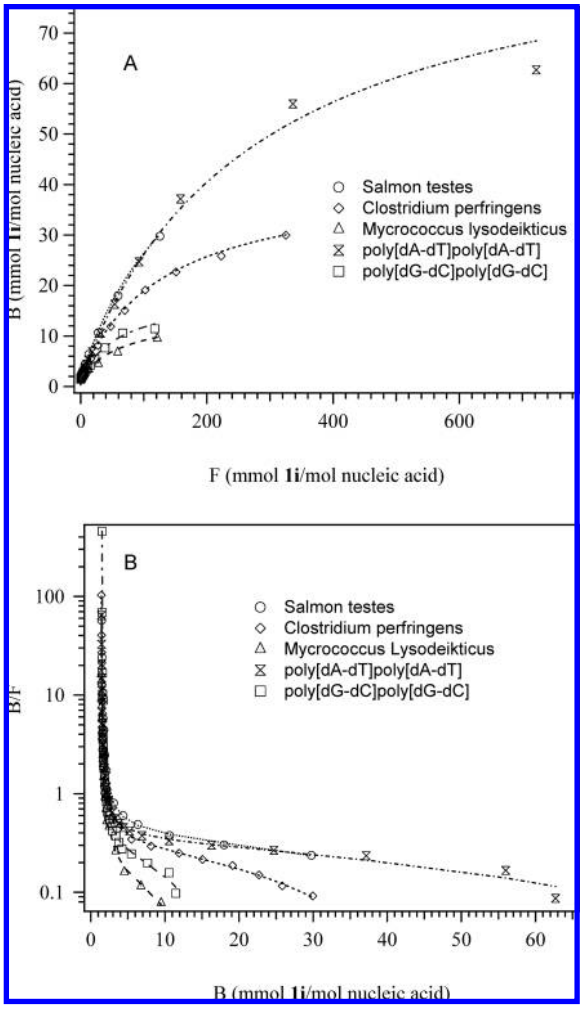

Figure 2. (A) Binding of **1i** to nucleic acids as a function of F quantity. (B) Binding analysis with the thermodynamic treatment of the Scatchard method. The experimental data (symbols) were fitted using the equation shown in Experimental Section, and the theoretical curves (lines) indicate the result of the fitting.

Molecular Modeling. To rationalize the biological results obtained with this new series of benzothiopyranoindoles, a molecular modeling study was carried out. Insight into the mode of binding of derivatives **1e**, **1i**, and **1p** to DNA and the stability of selected DNA duplex−intercalator complexes was gained through molecular docking and ab initio quantum mechanical calculations using the DNA hexamer $d(TATATA)_2$. This sequence was selected according to the experimental binding preference demonstrated for this type of compound in the fluorimetric determinations reported above. The DNA hexamer was obtained by molecular replacement using the crystal structure of deglycosylated pepleomycin bound to the self-complementary hexamer $d(\underline{CG}TA\underline{CG})_2$ as a starting model (PDB code 1a01)[45] with the d(CpG) base pairs (underlined) replaced with d(TpA) ones. Then pepleomycin was removed and the central d(TpA) intercalation site was utilized for docking simulations. Docking was carried out using the automated docking program AutoDock 4.0,[46] which allows torsional flexibility in the ligand and incorporates an efficient Lamarckian genetic search algorithm along with an empirical free energy function.

Out of a total of 200 independent docking runs, AutoDock provided well-clustered results, which were chosen according to the following criteria: (i) the most favorable docking energy (ΔG_{bind}), (ii) the highest frequency of occurrence (f_{occ}), and (iii) the formation of a direct intermolecular interaction between the alkyl-ammonium side chain of the ligand and DNA, as suggested by the SAR data. Docking results are summarized in Table 3, and a graphical representation of the binding modes of the most structurally representative derivatives **1e** and **1i** is given in Figure 3.

Two possible binding poses were found for the most active compounds **1e** and **1i**. As depicted in Figure 3, the planar benzothiopyranoindole moiety was sandwiched between adjacent A−T base pairs, while the charged side chain could sit equally well in major or minor groove. In solution 1 (ΔG_{bind} = −9.9 kcal/mol, f_{occ} = 22/200 for **1e**; ΔG_{bind} = −10.4 kcal/mol, f_{occ} = 65/200 for **1i**), the protonated

Table 3. Results of 200 Independent Docking Runs for Compounds **1e**, **1i**, **1p**, and Corresponding Binding Energies as Calculated by ab Initio Methods

	molecular docking			ab initio calculations		
compd	N_{tot}[a]	cluster[b]	$f_{occ.}$[c]	ΔG_{bind}[d]	ΔE_{bind}	ΔE_{bind} (PCM)
1e	10	1	22/200	−9.9	−162.84	−49.70
		2	22/200	−9.9	−151.11	−65.40
1i	8	1	65/200	−10.4	−163.87	−53.93
		2	55/200	−10.2	−184.58	−67.04
1p	16	1	39/200	−10.0	−153.98	−55.70

[a] N_{tot} is the total number of clusters. [b] The assessment of conformational cluster sizes was determined as a function of the root-mean-square deviation (rmsd) of 0.3 Å between conformers. [c] The number of results contained in the clusters is given by the frequency of occurrence, f_{occ}. [d] ΔG_{bind} is the estimated free energy of binding for the clusters. Energies are in kcal/mol.

Table 2. Binding Parameters for Compound **1i**

nucleic acid	B_{max} (mmol/mol nucleic acid)	B_{max1} (mmol/mol nucleic acid)	B_{max2} (mmol/mol nucleic acid)	k_1	k_2
poly[dA-dT]poly[dA-dT]	93.93(2)[a]	1.49(1)	92.44(2)	62.98(3)	0.0036(4)
Clostridium perfringens DNA	41.47(3)	1.57(4)	39.89(3)	31.40(6)	0.0076(3)
salmon testes DNA	68.89(4)	1.72(2)	67.17(3)	8.22(4)	0.0058(2)
Mycrococcus lysodeikticus DNA	14.81(3)	1.74(2)	13.06(4)	7.42(2)	0.013(3)
poly[dG-dC]poly[dG-dC]	18.32(6)	1.45(2)	16.87(3)	ND[b]	0.0157(2)

[a] Standard deviations in the least significant digits are given in parentheses. [b] Fitting not satisfactory. Not detected.

Downloaded by TATA INST OF FUNDAMENTAL RES on October 11, 2009 | http://pubs.acs.org
Publication Date (Web): August 19, 2009 | doi: 10.1021/jm900627v

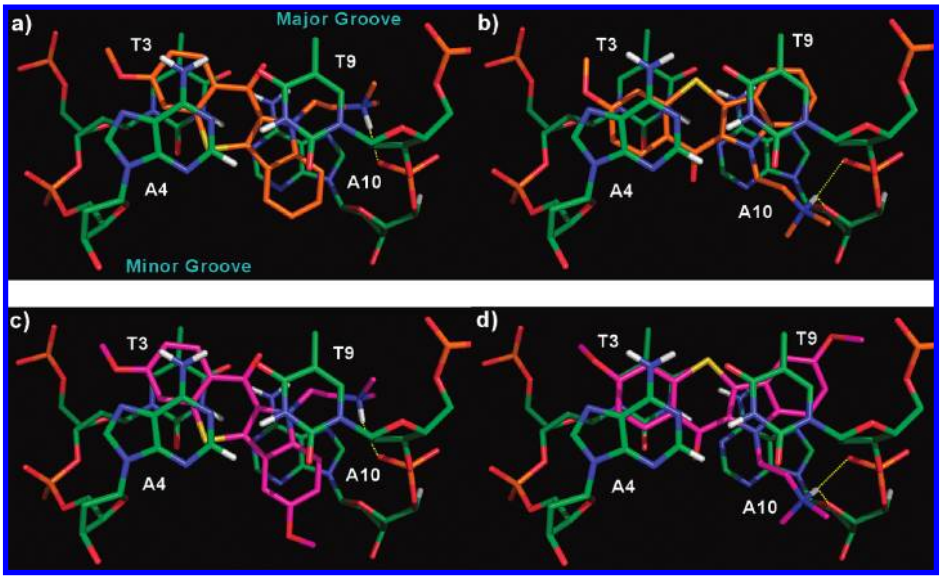

Figure 3. Intercalation site of the two complexes between compounds **1e** (orange, (a) and (b)) and **1i** (magenta, (c) and (d)) and hexamer $d(TATATA)_2$ viewed in a projection plane orthogonal to the helix axis. Left: complexes with the protonated dimethylammonium group in the major groove ((a) and (c)). Right: complexes with the protonated dimethylammonium group in the minor groove ((b) and (d)). Nonpolar hydrogens were removed for clarity. H-bonds are represented with yellow dashed lines.

dimethylammonium group of the side chain sat in the DNA major groove, participating in an ionic interaction with the negatively charged phosphate backbone of adenine A10 (Figure 3a,c). On the contrary, in solution 2 (ΔG_{bind} = −9.9 kcal/mol, f_{occ} = 22/200 for **1e**; ΔG_{bind} = −10.2 kcal/mol, f_{occ} = 55/200 for **1i**), the charged side chain projected into the minor groove, establishing H-bonds with both the deoxyribose O4′ and the phosphate backbone of adenine A10 (Figure 3b,d). Notably, in the latter case, a better superposition of the ligand benzothiopyranoindole moiety with the DNA base pairs is observed, suggesting stronger $\pi-\pi$ stacking interactions for this binding mode. Such a favorable arrangement seems to be determined by the length of the alkylammonium side chain, which is firmly anchored to the phosphate backbone in both solutions and drives the extended planar moiety into the DNA double helix.

A well-clustered binding pose was found by AutoDock for compound **1p** (f_{occ} = 39/200; ΔG_{bind} = −10.0 kcal/mol), which strongly resembled the solution 2 found for **1e** and **1i** (Figure 3b,d). The ligand was found to intercalate between the d(TpA) base pairs with the side chain protruding into the DNA minor groove, where the protonated diethylamino group engaged in H-bonding interactions with both the deoxyribose O4′ and the phosphate backbone of adenine A10. It is of note that the replacement of dimethylammonium by the diethylammonium group, as well as the introduction of a chlorine atom in X′, does not lead to significant changes in ΔG_{bind} when compared with **1e** and **1i**.

To estimate the binding energy of the DNA−ligand complexes more accurately, as well as the relative contribution of specific interactions ($\pi-\pi$ stacking, H-bonding, etc.) and the effects of substituents, we performed ab initio quantum mechanical calculations focusing on the most active compounds **1e**, **1i**, and **1p**. A full molecular mechanics minimization, keeping all degrees of freedom, of the five complex structures considered (two for **1e** and **1i**, and one for **1p**) was carried out with the AMBER 9 software package,[47] modeling the DNA hexamer and the ligands with the AMBER99[48] and GAFF[49] force fields, respectively. Solvent effects were

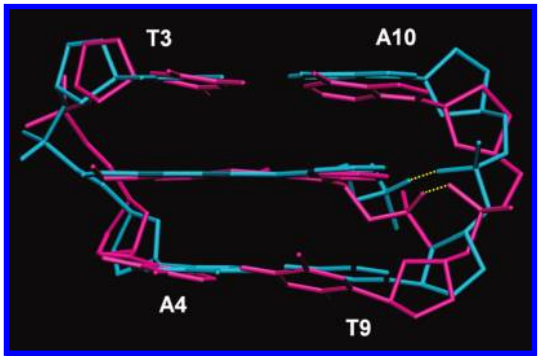

Figure 4. Binding orientation of compound **1e** in the DNA intercalation site, before (magenta) and after (cyano) energy-minimization. H-bonds are represented with yellow dashed lines.

also included using the generalized Born/surface area (GB/SA) model, as implemented in AMBER. In this step, the DNA−ligand structures underwent minor but still significant, rearrangements with respect to the docking structures. In particular, the aromatic moieties of the DNA base pairs assumed a more planar conformation with respect to the ligands, compatible with stronger $\pi-\pi$ stacking interactions and an overall better match of the ligands inside the DNA strands, as shown in Figure 4. In the second step, we performed quantum mechanical calculations on a relatively large fragment of the previously optimized DNA−ligand complexes, including the whole ligand and the two proximal nucleic acid base pairs with the connecting sugar rings and phosphate groups. Hydrogen atoms were added to cap the terminating oxygen atoms on the deoxyribose. On the basis of the above considerations, for such calculations we decided to rely on a well-trusted and effective density functional theory (DFT) based method, namely B3LYP,[50a,50b] using a medium size basis set, 6-31+G(d,p). Because of the known underestimation of the dispersion forces by DFT, a long-range correction term was included according to the scheme proposed by Grimme[51] and recently implemented[52] in a modified version of the Gaussian03 software package.[53]

Downloaded by TATA INST OF FUNDAMENTAL RES on October 11, 2009 | http://pubs.acs.org
Publication Date (Web): August 19, 2009 | doi: 10.1021/jm900627v

Downloaded by TATA INST OF FUNDAMENTAL RES on October 11, 2009 | http://pubs.acs.org
Publication Date (Web): August 19, 2009 | doi: 10.1021/jm900627v

Indeed, such correction has shown significant improvements in the treatment of aromatic ring interactions.[52] Finally, the effects of the aqueous environment were included via an implicit solvent model, the conductor-like version[54a,54b] of the polarizable continuum model (PCM).[55] Results on the binding energy, ΔE_{bind}, where $\Delta E_{bind} = \Delta E_{complex} - \Delta E_{DNA} - \Delta E_{ligand}$ of the complexes are reported in Table 3.

As expected, we noted that the solvent effect decreases the absolute binding energy by a significant amount (see ΔE_{bind} PCM), changing the relative order of the complex stability. Not surprisingly, the complexes between DNA and solution 2 of both **1e** and **1i** were the most stable ones. As noted above, we observed a strong H-bond between the dialkyl-ammonium chain and the negatively charged phosphate group and, more importantly, more favorable $\pi-\pi$ stacking interactions between the extended planar moiety of the ligands and the DNA bases, as shown in Figure 3. On the contrary, **1p**, which has a bulkier side chain, possessed a weaker interaction of the ammonium group with the DNA phosphate group. Therefore, the present results consistently support the same binding mode as the preferred one for the DNA intercalation of the most active compounds considered in this study, **1e** and **1i**.

To evaluate the possible contribution of other terms to the total binding energy with respect to the usual intermolecular interactions, e.g., $\pi-\pi$ stacking, H-bonding, etc., we computed the charge-transfer occurring between the ligand and the DNA base pairs. Considering the complex between solution 2 of **1e** and DNA, we obtained a net change of the total electrostatic charge of the ligand of less than 0.07 au in going from vacuum to the intercalation site, thus showing a negligible charge transfer, as found in previous computational studies of other intercalating compounds.[56] To proceed further, the fundamental role of the dialkyl-ammonium side chain was analyzed in terms of the decrease of the binding energy, ΔE_{bind}, after removing the cationic headgroup in the DNA/**1e** complex. By changing the $-(CH_2)_2NH^+(CH_3)_2$ side chain to a neutral and apolar terminal group (CH_2CH_3), we obtained a destabilization energy of the complex of about 24 kcal/mol, which amounts to almost 40% of the original binding energy. At the same time, this result confirms that the predominant contribution to the DNA/ligand binding is represented by the extended $\pi-\pi$ stacking interactions (about 60%). Note that the positively charged ammonium group not only significantly stabilizes the complex but also that it might play an important role in anchoring the ligand to the DNA duplex at the moment of complex formation, making the insertion of the planar moiety into the DNA intercalation site easier. Indeed, as observed in Table 1, when the dialkyl-ammonium side chain is elongated and/or becomes bulkier in comparison with **1e** and **1i**, the cytotoxic activity decreases in every case, with the exception of **1p**. Remarkably, this seems to be consistent with the proposed DNA−ligand binding mode, where the side chain specifically binds to the phosphate group, considering that a longer and more sterically hindered chain makes the present interaction less favorable.

The effect of the substituent group in position X was analyzed by replacing the methoxy group with a hydrogen and a chlorine atom. Results showed little change in ΔE_{bind} in both cases (X = H, ΔE_{bind} = −62.7 kcal/mol; X = Cl, ΔE_{bind} = −66.0 kcal/mol). Similarly, we observed a negligible difference in the binding energy by replacing the methoxy group in position X′ with chlorine in the complex between solution 2 of **1i** and DNA (X′ = CH_3O, ΔE_{bind} = −67.0 kcal/mol; X′ = Cl, ΔE_{bind} = −66.6 kcal/mol).

Effect on Topoisomerase Activity. DNA topoisomerases have been shown to be the molecular target of many anticancer drugs, including known DNA intercalators.[57] Thus, the ability of new benzothiopyranoindole derivatives to form an intercalative complex with DNA suggested that their antiproliferative effect might be related to the interference with nuclear enzymes involved in DNA processing, such as topoisomerases.[15]

Figure 5A shows the effect of **1i** and **1e** on the relaxation of plasmid pBR322 DNA, mediated by topoisomerase II. The supercoiled DNA (DNA) was converted to relaxed forms by the enzyme (Topo II). The inhibition by **1i** and **1e** on the relaxation activity was demonstrated by the appearance of supercoiled DNA and by a concurrent decrease in relaxed products in the presence of the enzyme. In detail, for both derivatives a dose-dependent effect is evident at concentration ranging from 1 to 5 μM; interestingly, the inhibition induced at the higher concentration (5 μM) is similar to that obtained by 8 μM *m*-AMSA (*m*-AMSA), which was used as reference drug. A comparison between **1i** and **1e** showed a lower inhibitory effect on enzyme activity for the first derivative, which was especially evident at 2.5 μM concentration. This behavior appears in accordance with the antiproliferative data reported in Table 1. The results of Table 1 further suggested a crucial contribution to the cytotoxicity of the dialkylaminoalkyl side chain and in particular pointed out to the unfavorable role of its length and hindrance. This effect is particularly clear within the **1e**−**h** group of derivatives, for both cell lines tested. On the basis of these considerations, it appeared interesting to evaluate the effects of **1e**−**h**, along with the parent compound **1a**, on topoisomerase II relaxation ability (Figure 5B). The occurrence of supercoiled DNA, indicative of inhibition of the enzyme activity, decreases from **1e** to **1h**, in agreement with the cellular effect. Regarding the unsubstituted **1a**, which showed no cellular effect up to 20 μM concentration, it stimulates a very low formation of supercoiled DNA like **1h**, but in contrast it shows the maintenance of the relaxed form as was observed with the enzyme alone. This result could be a consequence of the difference in their abilities to interact with DNA, which is negligible for **1a** and notable for **1h**, as evidenced by the LD spectra showed in Figure 1.

Many intercalative agents, such as adriamycin, *m*-AMSA, and mitoxantrone, which are able to stabilize a biological intermediate in topoisomerase II activity, also known as cleavage complex,[20,57,58] into a lethal one, are called topoisomerase II poisons. The occurrence of the cleavage complex can be demonstrated experimentally by the enzyme-dependent formation of linear DNA from supercoiled DNA. Figure 6A shows a cleavage complex assay performed in the presence of increasing concentrations of the most active derivative **1e** and 8 μM *m*-AMSA, which was used as a reference compound. The supercoiled pBR322 DNA (DNA lane) was relaxed by the catalytic activity of the enzyme (Topo II), and as expected, *m*-AMSA, a well-known topoisomerase II poison, induces the formation of a significant amount of linear DNA. The benzothiopyranoindole derivative **1e** also appears able to stabilize the formation of cleavage complexes, although at all concentrations tested (up to 20 μM) it induces less linear DNA formation than *m*-AMSA. Experiments performed with **1i** showed a very weak capacity to form linear DNA (results not shown). The

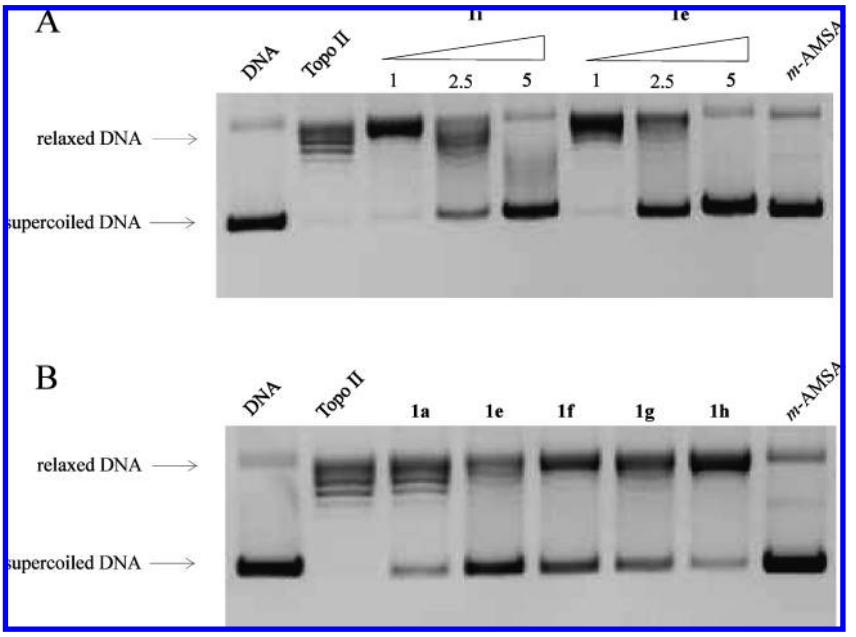

Figure 5. Effect on relaxation of supercoiled pBR322 DNA of human recombinant topoisomerase II. (A) Supercoiled DNA (DNA) was incubated with topoisomerase II in the absence (Topo II) and presence of **1i** and **1e** at indicated concentration (μM). Eight micromolar *m*-AMSA was used as reference. (B) Supercoiled DNA (DNA) was incubated with topoisomerase II in the absence (Topo II) and presence of **1a** and **1e**−**h** at 2.5 μM concentration; 8 μM *m*-AMSA was used as reference. The images are representative of three experiments.

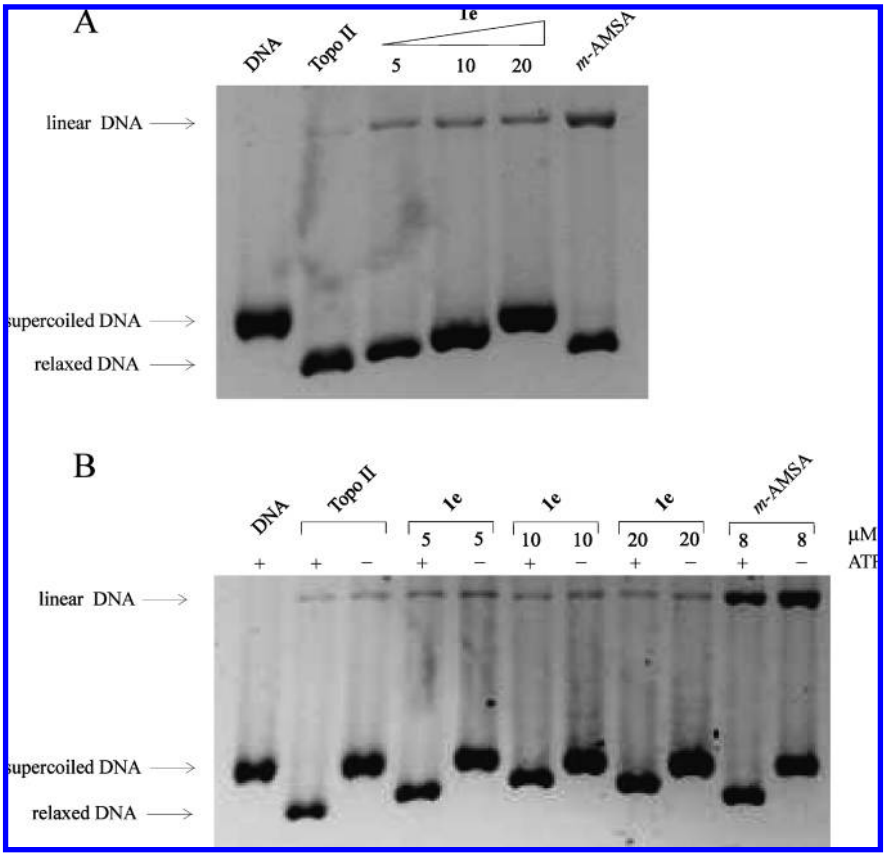

Figure 6. Effect of compound **1e** on the stabilization of covalent DNA-topoisomerase II complex. (A) Supercoiled pBR322 DNA (DNA) was incubated as reported in Experimental Section with topoisomerase II in the absence (Topo II) and presence of **1e** at indicated concentration (μM); 8 μM *m*-AMSA was used as reference. DNA samples were separated by electrophoresis on agarose gels containing 0.5 μg/mL ethidium bromide. (B) Experimental conditions as in (A), except where indicated (ATP). The images are representative of four experiments.

poisoning effect shown in Figure 6A appears quite weak with respect to the inhibition on topoisomerase II relaxation ability (Figure 5A), nevertheless, the same experiment, performed in the absence of ATP, to avoid any relaxation

Downloaded by TATA INST OF FUNDAMENTAL RES on October 11, 2009 | http://pubs.acs.org
Publication Date (Web): August 19, 2009 | doi: 10.1021/jm900627v

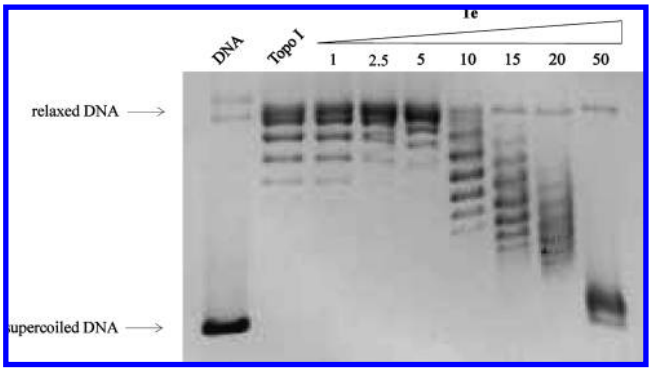

Figure 7. Effect of compound **1e** on relaxation of supercoiled pBR322 DNA by human recombinant topoisomerase I. Supercoiled DNA (DNA) was incubated with topoisomerase I in the absence (Topo I) and presence of **1e** at indicated concentrations (μM). The image is representative of three experiments.

Downloaded by TATA INST OF FUNDAMENTAL RES on October 11, 2009 | http://pubs.acs.org
Publication Date (Web): August 19, 2009 | doi: 10.1021/jm900627v

activity, confirmed the capacity of **1e** to induce the formation of linear DNA (Figure 6B). The topoisomerase II-mediated cleavage was further demonstrated by cleavage assay performed with end-labeled DNA in the presence of **1e** at 5 μM. By increasing the concentrations of **1e** up to 200 μM, a concurrent inhibition of the cleavage is observed and this behavior, typical of DNA intercalators,[59] confirms again the capacity of the new derivative to form an effective intercalative complex with DNA (see Supporting Information Figure S1).

To investigate the role of topoisomerase II on the antiproliferative effect exerted by **1e**, cell growth inhibition assay was performed by using HL-60/MX2 cells. These cells display altered topoisomerase II catalytic activity and reduced levels of topoisomerase II α and β and are approximately 30-fold less sensitive to *m*-AMSA and mitoxantrone than the HL-60 parental cells.[60] HL-60/MX2 cells incubated in the presence of the most active **1e** showed IC_{50} values ranging from 2.35 to 2.65 μM, thus indicating a degree of resistance, i.e., the ratio of the IC_{50} values calculated for resistant and sensitive cells (HL-60/MX2:HL-60), of about 6-fold.

The rather weak topoisomerase II poisoning effect, along with the obtained degree of resistance, suggest that, in addition to the inhibition on the topoisomerase II activity, other molecular events could contribute to the notable cytotoxicity induced by the new benzothiopyranoindoles. In particular, considering the significant intercalative capacity of the new compounds, a further interference with other DNA-related enzymes could occur.

On the basis of the above consideration and in view of the structural similarities of the investigated compounds with some dual topoisomerase I/II inhibitors, in particular the benzopyridoindole derivative Intoplicine,[61] the effect on the nuclear enzyme topoisomerase I was also assayed. Figure 7 shows the relaxation of supercoiled pBR322 DNA catalyzed by the topoisomerase I, in the presence of increasing amounts of **1e**. The addition of the benzothiopyranoindole derivative **1e** induces a concentration-dependent inhibition of the relaxation capacity and the effect becomes evident at 10 μM. A comparison between this result and that from topoisomerase II studies (shown in Figure 5) indicates a certain preference of action toward topoisomerase II. Indeed, while 5 μM of **1e** completely inhibits the relaxation catalyzed by this latter enzyme (Figure 5A), 1 order of magnitude higher of compound has to be used to evoke a comparable effect on topoisomerase I (Figure 7).

Conclusions

The synthesis of new benzothiopyranoindole derivatives carrying a dialkylaminoalkyl side group and exhibiting an antiproliferative effect at low micromolar concentrations on HeLa and HL-60 human cell lines was described. In particular, the chromophore scaffold itself (**1a**−**d**) does not possess any significant antiproliferative effect, even in the presence of substituents, such as a methoxy group or a chlorine atom in the 3 and/or 7 positions of the system; on the contrary, the presence of the dialkylaminoalkyl side chains, inserted at the 11-position on the indole nitrogen, seems to be required for the cytotoxicity (**1e**−**v**). In particular, the most notable effect was shown by the compound carrying a dimethylaminoethyl side chain, along with a methoxy group in the 7 position and hydrogen in the 3 position (**1e**), which is able to exert a cytotoxic effect higher than that of ellipticine on HL-60 cell line.

LD studies revealed that compounds **1e**−**v** are able to form a complex with DNA, which is consistent with an intercalative binding mode. Fluorimetric titrations in the presence of DNA characterized by different base compositions and synthetic polyDNAs interestingly, demonstrated a high sequence specificity of the benzothiopyranoindoles for AT rich regions. These studies allowed us to identify two binding sites, S_1 and S_2. The binding parameters permit the hypothesis that S_1 participates in a binding event independent of base composition and mediated by the charged side chain, while S_2 accounts for an intercalative complexation to AT rich regions, mediated by weak interactions. Molecular docking and high level quantum-mechanical calculations, including implicit solvent and a proper treatment of dispersion forces, allowed a further understanding at the molecular level of which specific interactions provide an optimal intercalative model, in agreement with experimental data, for the ligand−DNA complexes of the three most active compounds **1e**, **1i**, and **1p**. This model showed a strong ion pair interaction between the protonated dimethylaminoethyl side chain and the phosphate backbone (about 40% of ΔE_{bind}), with the side chain sitting in the DNA minor groove, and an extended $\pi-\pi$ stacking interaction between the benzothiopyranoindole moiety and the two adjacent DNA base pairs (about 60% of ΔE_{bind}). Hence, the crucial presence of the dialkylaminoalkyl side chain for achieving significant cytotoxic effects was corroborated by the present model, which also suggests that the side chain may play the important role of favoring the complex formation by anchoring the ligand firmly to the DNA during the insertion of the benzothiopyranoindole moiety into the nucleic acid strands.

The ability of the new 11-substituted benzothiopyranoindoles to intercalate between DNA base pairs prompted further investigations into possible interference with the activity of the nuclear enzymes topoisomerases I and II. The derivatives showed the capacity to inhibit the relaxation of supercoiled plasmid DNA mediated by topoisomerase II in a dose-dependent manner, and interestingly, this ability appeared in accordance with the antiproliferative data. Moreover, for the most cytotoxic derivative **1e**, a weak topoisomerase II poisoning effect and the capacity to inhibit the topoisomerase I-mediated DNA relaxation, was also demonstrated.

In conclusion, the ability to intercalate effectively between AT rich regions of nucleic acids, together with a noteworthy cytotoxic effect, render this new 11-substituted heteropolycyclic

Downloaded by TATA INST OF FUNDAMENTAL RES on October 11, 2009 | http://pubs.acs.org
Publication Date (Web): August 19, 2009 | doi: 10.1021/jm900627v

moiety a very interesting structure inside the field of DNA-targeted antiproliferative agents. Further modifications of both the 7 or/and 3 position of the tetracyclic chromophore and of the geometry of the distal end of the protonable side chains could improve the biological properties, thus allowing the development of new potential antitumor drugs.

Experimental Section

Chemistry. Melting points were determined using a Reichert Kofler hot-stage apparatus and are uncorrected. Infrared spectra (IR) were obtained on a NICOLET/AVATAR, 360 FT spectrophotometer as Nujol mulls. Nuclear magnetic resonance spectra (^{1}H NMR) were recorded on a Varian Gemini 200 spectrometer in DMSO-d_6 solution using TMS as the internal standard. Coupling constants are given in Hz. Magnesium sulfate was always used as the drying agent. Evaporations were made in vacuo (rotating evaporator). Analytical thin-layer chromatography (TLC) was carried out on Merck 0.2 mm precoated silica gel aluminum sheets (60 F-254). Reagents, starting materials, and solvents were purchased from commercial suppliers and used as received. Combustion analyses on target compounds were performed by our Analytical Laboratory in Pisa. All compounds showed ≥95% purity.

General Procedure for the Synthesis of 7-Methoxy-2,3-dihydro-3-*p*-substituted-phenylhydrazonobenzo[3′,2′:5,6]thiopyran-4(4*H*)-ones 3a−c and 7-Chloro derivative 3d. To a solution of 4.5 mmol of compound **2a** or **2b** in 30 mL of methanol was added an aqueous saturated solution of 14.0 mmol of sodium acetate. After cooling at 0 °C, a solution of the suitable diazonium salt, obtained from the appropriately *p*-substituted aniline in 18% hydrochloridric acid and sodium nitrite, was added dropwise in slight excess (6.0 mmol). An orange precipitate was immediately formed, and the mixture was stirred for 30 min at room temperature. The solid was collected and washed with water to give crude compounds **3a−d**, whose purity was assessed by TLC analysis (Supporting Information Tables 1−2).

General Procedure for the Synthesis of 7-Methoxy-3-substituted Benzo[3′,2′:5,6]thiopyrano[3,2-*b*]indol-10(11*H*)-ones 1a−c and 7-Chloro-Benzo[3′,2′:5,6]thiopyrano[3,2-*b*]indol-10(11*H*)-one 1d. A solution of 4 mmol of the suitable *p*-substituted phenylhydrazono derivative **3a−d** in 20 mL of ethanolic hydrogen chloride solution was refluxed for 20 min. After cooling the yellow/light-brown precipitate was collected and washed with ethanol to give crude indoles **1a−d**, which were purified by crystallization (Supporting Information Tables 3−4).

General Procedure for the Synthesis of 3,7-Substituted 11-Dialkylaminoalkyl-benzo[3′,2′:5,6]thiopyrano[3,2-*b*]indol-10(11H)-ones 1e−v. 0.70 mmol of the appropriate compound **1a−d** was added in small portions to a stirred suspension of sodium hydride in 60% dispersion in mineral oil (0.104 g, 2.60 mmol) in 10 mL of anhydrous DMF, under nitrogen atmosphere. The reaction mixture was stirred at room temperature for 2 h and then supplemented with 1.03 mmol of the appropriate dialkylaminoalkyl iodide hydroiodide and left at room temperature for 24 h; then the mixture was heated at 100 °C for 12−24 h (TLC analysis). After cooling, the reaction mixture was diluted with water and left to stand at room temperature overnight. The crude products precipitated were collected and purified by crystallization from DMF (Supporting Information Tables 5−12).

Inhibition Growth Assay. HL-60 (human myeloid leukemic cells) and HeLa (human cervix adenocarcinoma cells) were grown in RPMI 1640 (Sigma Chemical Co.) supplemented with 15% heat-inactivated fetal calf serum (Biological Industries) and in Nutrient Mixture F-12 [HAM] (Sigma Chemical Co.) supplemented with 10% heat-inactivated fetal calf serum (Biological Industries), respectively. HL-60/MX2 cells (ATCC, Manassas, Va) were grown in RPMI 1640 supplemented with 10% heat-inactivated fetal calf serum. 100 U/mL penicillin, 100 μg/mL streptomycin, and 0.25 μg/mL amphotericin B (Sigma Chemical Co.) were added to the media. The cells were cultured at 37 °C in a moist atmosphere of 5% carbon dioxide in air.

HL-60 and HL-60/MX2 cells (4×10^4) were seeded into each well of a 24-well cell culture plate. After incubation for 24 h, various concentrations of the test agents were added to the complete medium and incubated for a further 72 h. HeLa (4×10^4) cells were seeded into each well of a 24-well cell culture plate. After incubation for 24 h, the medium was replaced with an equal volume of fresh medium, and various concentrations of the test agents were added. The cells were then incubated in standard conditions for a further 72 h.

A trypan blue assay was performed to determine cell viability. Cytotoxicity data were expressed as IC_{50} values, i.e., the concentration of the test agent inducing 50% reduction in cell number compared with control cultures.

The degree of resistance is expressed as the ratio of the IC_{50} values calculated for resistant and sensitive cells (HL-60/MX2: HL-60).

Nucleic Acids. Salmon testes DNA (cat. D-1626, AT% about 60) was purchased from Sigma Chemical Company. Its hypochromicity, determined according to Marmur and Doty,[62] was over 35%. DNA from *Micrococcus lysodeikticus* (cat. D-8259, AT% about 30%) and *Clostridium perfringens* (cat. D-1760, AT% about 70), poly[dA-dT]·poly[dA-dT] (cat. D-0883), and poly[dG-dC]·poly[dG-dC] (cat. D-9389) also came from Sigma. pBR322 DNA was purchased from Fermentas Life Sciences.

Linear Flow Dichroism. LD measurements were performed on a Jasco J500A circular dichroism spectropolarimeter converted for LD and equipped with an IBM PC and a Jasco J interface.

Linear dichroism is defined as:

$$LD_{(\lambda)} = A_{\parallel(\lambda)} - A_{\perp(\lambda)}$$

where $A_\parallel$ and $A_\perp$ correspond to the absorbances of the sample when polarized light is oriented parallel or perpendicular to the flow direction, respectively. The orientation is produced by a device designed by Wada and Kozawa[63] at a shear gradient of 500−700 rpm and each spectrum was accumulated four times.

A solution of salmon testes DNA (1.9×10^{-3} M) in ETN buffer (containing 10 mM TRIS, 10 mM NaCl, and 1 mM EDTA, pH = 7) was used. Spectra were recorded at 25 °C at different [drug]/[DNA] ratios.

Fluorimetric Determinations. Fluorescence spectra were recorded on a Jasco FP-6500 fluorescence spectrophotometer equipped with a stirred Peltier thermostatted cell holder at λ_{ecc} = 341 nm. Experiments were performed by addition of small amounts of free ligand to a solution containing nucleic acid−ligand complex at [nucleic acid]/[drug] = 700. The fluorescence emission of the complex is significantly higher with respect to that of free ligand. The concentration of the free ligand was the same as that of the complex: in this way different [nucleic acid]/[drug] were obtained at a constant ligand concentration. All measurements were carried out in ETN buffer at 25 °C. The amounts of bound and free ligand were determined from emission reading at a fixed wavelength, corresponding to the maximum of emission, in accordance with the equations:

$$f_i = (F_i - F_0)/(F_{max} - F_0)$$

$$B = f_i[\text{compound}]$$

$$B_n = B/[\text{nucleic acid}]$$

$$F = (1 - f_i)[\text{compound}]$$

$$F_n = F/[\text{nucleic acid}]$$

where F_i is the ith emission fluorescence, F_0 is the emission fluorescence of the free compound, F_{max} is the emission

fluorescence of the complex, B is the ith concentration of bound, B_n is the ith concentration of bound normalized to the nucleic acid concentration, F is the ith concentration of free, and F_n is the ith concentration of free normalized to the nuclei acid concentration.

Binding Parameters. The binding data were evaluated by applying a thermodynamic treatment of ligand−receptor interactions.[44] Scatchard analysis was performed using the following equation:

$$\frac{[B]}{[F]} = \sum_{i=1}^{s}\{[B_{\max,i}] - [B_i]\}\left[\frac{1}{K_{i,1(t)}} + \varepsilon_i(F)\right]$$

where

$$\varepsilon_i(F) = \sum_{k=2}^{n_i} \frac{[F]^{k-1}}{\prod_{j=1}^{k} K_{i,j}(t)}$$

The quantity $\varepsilon_i(F)$ represents an appropriate measure of the extent of multiple coordination on the ith site. $[B_{\max,i}]$ is the maximum concentration of the ith site that may be bound by the ligand, $[B_i]$ is the concentration of ith sites bound by the ligand, $[B_{\max}]$ is the maximum receptor-bound ligand concentration, $[F]$ is the free ligand concentration, $K_{i,j}(t)$ is the affinity constant of the ligand for the ith site, j is the occupancy number, and t is time. Fitting was performed using Igor pro 5.0.4.8 program.

Computational Chemistry. Molecular modeling and graphics manipulations were performed using the Maestro Graphical User Interface version 8.0.314 for Linux operating systems,[64a,64b] running it on a quad-core QX 6700 processor (8GB RAM). Model building and energy minimizations of compounds **1e**, **1i**, and **1p** were realized by employing the MacroModel 9.0 module of Maestro selecting the OPLS_2005 force field.[65a,65b] Pymol version 0.9[66] were used to create Figures 3 and 4.

Ligand and DNA Setup. The core structure of compounds **1e**, **1i**, and **1p** were retrieved from the Cambridge Structural Database (CSD)[67] and modified by using standard bond lengths and bond angles of the fragment library of Maestro. Geometry optimizations were realized with the Polak−Ribière conjugate gradient (PRCG) method until a convergence to the gradient threshold of 0.05 kJ/(mol Å). The atomic charges were computed using the OPLS_2005 force field. The compounds were considered in their protonated form.

The $d(TATATA)_2$ hexamer was built by molecular replacement using as a starting model the crystal structure of deglycosylated pepleomycin bound to the self-complementary hexamer $d(CGTACG)_2$ (PDB code 1a01).[45] Pepleomycin was then removed and the central d(TpA) intercalation site was utilized for docking experiments.

Docking Studies. Docking simulations for **1e**, **1i**, and **1p** were carried out by means of the AutoDock software (version 4.0).[68a,68b] To search the low-energy docked conformation of the ligand on the DNA, the empirical free energy function and the Lamarckian genetic algorithm were used. In this approach, the ligand performs a random walk around the static nucleic acid. At each time step, the ligand is moved by small increments in global translation and orientation at each of the rotational torsion angles. Depending on the input parameter values for the number of generations and the total number of energy evaluations, configurations are generated for grid points on the nucleic acid surface. The energy of the configurations is calculated based on a previously defined grid surface. Interaction energies are calculated with a free-energy-based expression. The docked energies are listed in increasing order of energy.

For the DNA hexamer, polar hydrogens were added and Kollman charges were assigned, whereas the Gasteiger−Marsili partial charges were used for the ligands. The ligand binding site was defined using a grid map of 60 × 60 × 60 points (Å^3), centered on the central d(TpA) intercalation site, with 0.375 Å grid-point spacing applying a standard protocol with an initial population of 150 randomly placed individuals and a maximum number of 2.5×10^7 energy evaluations per run. All other parameters were maintained at their default settings. A total of 200 binding conformations were carried out for each ligand generated by the program and then clusterized by means of AutoDock Tools.[68a,68b] Cutoffs for clustering were set at 0.8 Å rmsd and were represented by the result with the most favorable free energy binding (ΔG_{bind}). The fitness score is taken as the negative of the sum of the energy terms so that larger fitness scores indicate a better binding. The docked structures were analyzed using AutoDock Tools for hydrogen bonding and hydrophobic interactions.

Molecular Mechanics Optimizations and ab Initio Calculations. Selected complexes of the DNA hexamer with the **1e**, **1i**, and **1p** were further optimized at molecular mechanics (MM) level by using the AMBER 9 software package,[47] including solvent effects via the generalized Born/surface area (GB/SA) model. The general AMBER force field (GAFF),[49] specifically developed for rational drug design, was employed to model the ligands and, for consistency, the corresponding atomic charges were computed by using the quantum mechanical RESP charge method at HF/6-31G* level. The DNA fragment was modeled according to the AMBER-99 force field and molecular optimizations were performed with the steepest descent method, switching to the conjugate gradient method every 100 cycles. Once optimized at MM level, full ab initio calculations were carried out at B3LYP/6-31+G(d,p) level of the complexes formed between the intercalating ligands and the two proximal nucleic acid base pairs, including the chemically relevant deoxyribose and phosphate groups (see Figure 4). Solvent effects were eventually included using the conductor-like version[54a,54b] of the polarizable continuum model.[55] Because of the generally poor description of van der Waals interactions by DFT based methods, we included long-range corrections of the London dispersion forces according to the scheme proposed by Grimme.[51] All quantum mechanical calculations were performed with a modified version[52] of the Gaussian03 software package.[53]

Topoisomerases-Mediated DNA Relaxation. Supercoiled pBR322 plasmid DNA (0.25 μg, Fermentas Life Sciences) was incubated with 1U topoisomerase II (human recombinant topoisomerase II α, USB) or 2U topoisomerase I (calf thymus topoisomerase I, USB) and the test compounds as indicated for 60 min at 37 °C in 20 μL of reaction buffer.

Reactions were stopped by adding 4 μL of stop buffer (5% sodium dodecyl sulfate (SDS), 0.125% bromophenol blue, and 25% glycerol) and 50 μg/mL proteinase K (Sigma) and incubating for a further 30 min at 37 °C. The samples were separated by electrophoresis on a 1% agarose gel at room temperature. The gels were stained with ethidium bromide 1 μg/mL in TAE buffer (0.04 M Tris-acetate and 0.001 M EDTA), transilluminated by UV light, and fluorescence emission was visualized by a CCD camera coupled to a Bio-Rad Gel Doc XR apparatus.

Topoisomerase II-Mediated DNA Cleavage. Reaction mixtures (20 μL) containing 10 mM Tris-HCl (pH = 7.9), 50 mM NaCl, 50 mM KCl, 5 mM $MgCl_2$, 0.1 mM EDTA, 15 μg/mL bovine serum albumine (BSA), 1 mM ATP, 0.25 μg pBR322 plasmid DNA, 10 U topoisomerase II (human recombinant topoisomerase II α, USB), and test compounds were incubated for 60 min at 37 °C. Reactions were stopped by adding 4 μL of stop buffer (5% SDS, 0.125% bromophenol blue and 25% glycerol) and 50 μg/mL proteinase K (Sigma) and incubating for a further 30 min at 37 °C. The samples were separated by electrophoresis on a 1% agarose gel containing ethidium bromide 0.5 μg/mL at room temperature in TBE buffer (0.09 M Tris-borate and 0.002 M EDTA).

Downloaded by TATA INST OF FUNDAMENTAL RES on October 11, 2009 | http://pubs.acs.org
Publication Date (Web): August 19, 2009 | doi: 10.1021/jm900627v

Acknowledgment. This work was supported by MIUR (cofin 2006).

Supporting Information Available: Tables including physical properties, analytical, and spectral data of compounds **1a**−**v** and **3a**−**d**. Results and experimental procedure for topoisomerase II-mediated cleavage of end-labeled DNA induced by **1e**. This material is available free of charge via the Internet at http://pubs.acs.org.

References

(1) Parkin, D. M. Global cancer statistics in the year 2000. *Lancet Oncol*. **2001**, *2*, 533–543.
(2) Schwartsmann, G.; Ratain, M. J.; Cragg, G. M.; Wong, J. E.; Saijo, N.; Parkinson, D. R.; Fujiwara, Y.; Pazdur, R.; Newman, D. J.; Dagher, R.; Di Leone, L. Anticancer Drug Discovery and Development Throughout the World. *J. Clin. Oncol*. **2002**, *20*, 47s–59s.
(3) Neidle, S.; Thurston, D. E. Chemical approaches to the discovery and development of cancer therapies. *Nat. Rev. Cancer* **2005**, *5*, 285–296.
(4) Pujol, M. D.; Romero, M.; Sanchez, I. Synthesis and Biological Activity of New Class of Dioxygenated Anticancer Agents. *Curr. Med. Chem. Anticancer Agents* **2005**, *5*, 215–237.
(5) Hurley, L. H. DNA and its associated processes as targets for cancer therapy. *Nature Rev. Cancer* **2002**, *2*, 188–200.
(6) Zhou, B-B. S.; Bartek, J. Targeting the checkpoint kinases: chemosensitization versus chemoprotection. *Nat. Rev. Cancer* **2004**, *4*, 216–225.
(7) Borowski, E.; Shugar, D. In *Molecular Aspects of Chemotherapy*; Pergamon Press: New York, 1991; pp 105−118.
(8) Brana, M. F.; Cacho, M.; Gradillas, A.; Ramos, A. Intercalators as Anticancer Drugs. *Curr. Pharm. Des*. **2001**, *7*, 1745–1780.
(9) Bischoff, G.; Hoffmann, S. DNA-Binding of Drugs Used in Medicinal Therapies. *Curr. Med. Chem*. **2002**, *9*, 321–348.
(10) Denny, W. A. DNA-intercalating ligands as anti-cancer drugs: prospects for future design. *Anti-Cancer Drug Des*. **1989**, *4*, 241–263.
(11) Wang, J. C. DNA topoisomerases as targets of therapeutics: an overview. In *Advances in Pharmacology*; Liu, L. F., Ed.; Academic Press: New York, 1994; 29A, pp 1−19.
(12) Osheroff, N.; Corbett, A. H.; Robinson, M. J. Mechanism of action of topoisomerase II-targeted antineoplastic drugs. *Adv. Pharmacol. B* **1994**, *29*, 105–126.
(13) Capranico, G.; Zunino, F. DNA topoisomerase-trapping antitumour drugs. *Eur. J. Cancer* **1992**, *28A*, 2055–2060.
(14) Gale, K. C.; Osheroff, N. Uncoupling the DNA cleavage and relegation activities of topoisomerase II with a single-stranded nucleic acid substrate: evidence for an active enzyme-cleaved DNA intermediate. *Biochemistry* **1990**, *29*, 9538–9545.
(15) Wang, J. C. Cellular roles of DNA topoisomerases: a molecular perspective. *Nat. Rev. Mol. Cell. Biol*. **2002**, *3*, 430–440.
(16) Redinbo, M. R.; Stewart, L.; Kuhn, P.; Champoux, J. J.; Hol, W. G. Crystal Structures of Human Topoisomerase I in Covalent and Noncovalent Complexes with DNA. *Science* **1998**, *279*, 1504–1513.
(17) Leppard, J. B.; Champoux, J. J. Human DNA topoisomerase I: relaxation, roles and damage control. *Chromosoma* **2005**, *114*, 75–85.
(18) Schoeffler, A. J.; Berger, J. M. Recent advances in understanding structure−function relationships in the type II topoisomerase mechanism. *Biochem. Soc. Trans*. **2005**, *33*, 1465–1470.
(19) Nitiss, J. L. DNA topoisomerase II and its growing repertoire of biological functions. *Nat. Rev. Cancer* **2009**, *9*, 327–337.
(20) Liu, L. F. DNA topoisomerase poisons as antitumor drugs. *Annu. Rev. Biochem*. **1989**, *58*, 351–375.
(21) Denny, W. A. Dual topoisomerase I/II poisons as anticancer drugs. *Expert Opin. Invest. Drugs* **1997**, *6*, 1845–1851.
(22) Pommier, Y.; Tanizawa, A.; Kohn, K. W. Mechanisms of topoisomerase I inhibition by anticancer drugs. In *Advances in Pharmacology*; Liu L. F., Ed.; Academic Press: New York, 1994; Vol. 29B, pp 73−92.
(23) Holden, J. A. DNA Topoisomerases as Anticancer Drug Targets: From the Laboratory to the Clinic. *Curr. Med. Chem. Anticancer Agents* **2001**, *1*, 1–25.
(24) Larsen, A. K.; Escargueil, A. E.; Skladanowski, A. Catalytic topoisomerase II inhibitors in cancer therapy. *Pharmacol. Ther*. **2003**, *99*, 167–181.
(25) Pommier, Y. Topoisomerase I inhibitors: camptothecins and beyond. *Nat. Rev. Cancer* **2006**, *6*, 789–802.
(26) Nitiss, J. L. Targeting DNA topoisomerase II in cancer chemotherapy. *Nat. Rev. Cancer* **2009**, *9*, 338–350.
(27) Cozzi, P.; Mongelli, N.; Suarato, A. Recent Anticancer Cytotoxic Agents. *Curr. Med. Chem.—Anti-Cancer Agents* **2004**, *4*, 93–121.
(28) Lown, J. W., Ed. *Anthracycline and Anthracenedione-Based Anticancer Agents*; Elsevier Science: NewYork, 1988; p 402.
(29) Beretta, G. L.; Perego, P.; Zunino, F. Mechanisms of cellular resistance to camptothecins. *Curr. Med. Chem*. **2006**, *13*, 3291–3305.
(30) Ryckebusch, A.; Garcin, D.; Lansiaux, A.; Goossens, J. F.; Baldeyrou, B.; Houssin, R.; Bailly, C.; Hénichart, J. P. Synthesis, Cytotoxicity, DNA Interaction, and Topoisomerase II Inhibition Properties of Novel Indeno[2,1-*c*]quinolin-7-one and Indeno[1,2-*c*]isoquinolin-5,11-dione Derivatives. *J. Med. Chem*. **2008**, *51* (12), 3617–3629.
(31) Jiménez-Alonso, S.; Chávez Orellana, H.; Estévez-Braun, A.; G. Ravelo, A.; Pérez-Sacau, E.; Machín, F. Design and Synthesis of a Novel Series of Pyranonaphthoquinones as Topoisomerase II Catalytic Inhibitors. *J. Med. Chem*. **2008**, *51*, 6761–6772.
(32) Teicher, B. A. Next generation topoisomerase I inhibitors: rationale and biomarker strategies. *Biochem. Pharmacol*. **2008**, *75*, 1262–1271.
(33) Xie, L.; Qian, X.; Cui, J.; Xiao, Y.; Wang, K.; Wu, P.; Cong, L. Novel angular furoquinolinones bearing flexible chain as antitumor agent: design, synthesis, cytotoxic evaluation, and DNA-binding studies. *Bioorg. Med. Chem*. **2008**, *16*, 8713–8718.
(34) Bailly, C. Topoisomerase I Poisons and Suppressors as Anticancer Drugs. *Curr. Med. Chem*. **2000**, *7*, 39−58 and references therein.
(35) Baguley, B. C. DNA intercalating anti-tumour agents. *Anti-Cancer Drug Des*. **1991**, *6*, 1–35.
(36) Capranico, G.; Zunino, F. Antitumor Inhibitors of DNA Topoisomerases. *Curr. Pharm. Des*. **1995**, *1*, 1–14.
(37) Da Settimo, A.; Da Settimo, F.; Marini, A. M.; Primofiore, G.; Salerno, S.; Viola, G.; Dalla Via, L.; Marciani Magno, S. Synthesis, DNA binding and in vitro antiproliferative activity of purinoquinazoline, pyridopyrimidopurine and pyridopyrimidobenzimidazole derivatives as potential antitumor agents. *Eur. J. Med. Chem*. **1998**, *33*, 685–696.
(38) Dalla Via, L.; Gia, O.; Marciani Magno, S.; Da Settimo, A.; Marini, A. M.; Primofiore, G.; Da Settimo, F.; Salerno, S. Synthesis, in vitro antiproliferative activity and DNA-interaction of benzimidazoquinazoline derivatives as potential anti-tumor agents. *Il Farmaco* **2001**, *56*, 159–167.
(39) Dalla Via, L.; Gia, O.; Marciani Magno, S.; Da Settimo, A.; Primofiore, G.; Simorini, F.; Marini, A. M.; Da Settimo, F. Dialkylaminoalkylindolonaphthyridines as potential antitumour agents: synthesis, cytotoxicity and DNA binding properties. *Eur. J. Med. Chem*. **2002**, *37*, 475–486.
(40) Dalla Via, L.; Marini, A. M; Salerno, S.; Toninello, A. Mitochondrial permeability transition induced by novel pyridothiopyranopyrimidine derivatives: potential new antimitochondrial antitumour agents. *Biochem. Pharmacol*. **2006**, *72*, 1657–1667.
(41) Dalla Via, L.; Marini, A. M.; Salerno, S.; La Motta, C.; Condello, M.; Arancia, G.; Agostinelli, E.; Toninello, A. Synthesis and biological activity of 1,4-dihydrobenzothiopyrano[4,3-*c*]pyrazole derivatives, novel pro-apoptotic mitochondrial targeted agents. *Bioorg. Med. Chem*. **2009**, *17*, 326–336.
(42) Phillips, R. R. *Org. Reactions* **1959**, *10*, 143–178.
(43) Marechal, R.; Bagot, J. Muscarine-like action of some halogenated derivatives of alkyltrimethylammoniums (homologs of bromocholine). II. Chemistry. *Ann. Pharm. Fr*. **1946**, *4*, 172–181.
(44) (a) Di Noto, V.; Dalla Via, L.; Toninello, A.; Vidali, M. Thermodynamic treatment of ligand−receptor interactions. *Macromol. Theory Simul*. **1996**, *5*, 165–181. (b) Di Noto, V.; Dalla Via, L.; Zatta, P. Review of binding methods and detection of Al(III) binding events in trypsin and DL-DPPC liposomes by a general thermodynamic model. *Coord. Chem. Rev*. **2002**, *228*, 343–363.
(45) Caceres-Cortes, J.; Sugiyama, H.; Ikudome, K.; Saito, I.; Wang, A. H.-J. Interactions of Deglycosylated Cobalt(III)-Pepleomycin (Green Form) with DNA Based on NMR Structural Studies. *Biochemistry* **1997**, *36*, 9995–10005.
(46) Morris, G. M.; Goodsell, D. S.; Halliday, R. S.; Huey, R.; Hart, W. E.; Belew, R. K.; Olson, A. J. Automated Docking Using a Lamarckian Genetic Algorithm and an Empirical Binding Free Energy Function. *J. Comput. Chem*. **1998**, *19*, 1639–1662.
(47) Case, D. A.; Darden, T. A.; Cheatham, T. E., III; Simmerling, C. L.; Wang, J.; Duke, R. E.; Luo, R.; Merz, K. M.; Pearlman, D. A.; Crowley, M.; Walker, R. C.; Zhang, W.; Wang, B.; Hayik, S.; Roitberg, A.; Seabra, G.; Wong, K. F.; Paesani, F.; Wu, X.; Brozell, S.; Tsui, V.; Gohlke, H.; Yang, L.; Tan, C.; Mongan, J.; Hornak, V.; Cui, G.; Beroza, P.; Mathews, D. H.; Schafmeister, C.;

Downloaded by TATA INST OF FUNDAMENTAL RES on October 11, 2009 | http://pubs.acs.org
Publication Date (Web): August 19, 2009 | doi: 10.1021/jm900627v

Ross, W. S.; Kollman, P. A. *AMBER, version 9*; University of California: San Francisco, CA, 2006.
(48) Wang, J. M.; Cieplak, P.; Kollman, P. A. How well does a restrained electrostatic potential (RESP) model perform in calculating conformational energies of organic and biological molecules? *J. Comput. Chem.* **2000**, *21*, 1049–1074.
(49) Wang, J.; Wolf, R. M.; Caldwell, J. W.; Kollman, P. A.; Case, D. A. Development and testing of a general Amber force field. *J. Comput. Chem.* **2004**, *25*, 1157–1174.
(50) (a) Becke, A. D. Density-functional thermochemistry. III. The role of exact exchange. *J. Chem. Phys.* **1993**, *98*, 5648–5652. (b) Stephens, P. J.; Devlin, F. J.; Chabalowski, C. F.; Frisch, M. J. Ab initio calculation of vibrational absorption and circular dichroism spectra using density functional force fields. *J. Phys. Chem.* **1994**, *98*, 11623–11627.
(51) Grimme, S. Improved Second-Order Møller-Plesset Perturbation Theory by Separate Scaling of Parallel- and Antiparallel-Spin Pair Correlation Energies. *J. Chem. Phys.* **2003**, *118*, 9095–9102.
(52) Pavone, M.; Rega, N.; Barone, V. Implementation and validation of DFT-D for molecular vibrations and dynamics: The benzene dimer as a case study. *Chem. Phys. Lett.* **2008**, *452*, 333–339.
(53) Frisch, M. J.; Trucks, G. W.; Schlegel, H. B.; Scuseria, G. E.; Robb, M. A.; Cheeseman, J. R.; Montgomery, J., J. A.; Vreven, T.; Kudin, K. N.; Burant, J. C.; Millam, J. M.; Iyengar, S. S.; Tomasi, J.; Barone, V.; Mennucci, B.; Cossi, M.; Scalmani, G.; Rega, N.; Petersson, G. A.; Nakatsuji, H.; Hada, M.; Ehara, M.; Toyota, K.; Fukuda, R.; Hasegawa, J.; Ishida, M.; Nakajima, T.; Honda, Y.; Kitao, O.; Nakai, H.; Klene, M.; Li, X.; Knox, J. E.; Hratchian, H. P.; Cross, J. B.; Bakken, V.; Adamo, C.; Jaramillo, J.; Gomperts, R.; Stratmann, R. E.; Yazyev, O.; Austin, A. J.; Cammi, R.; Pomelli, C.; Ochterski, J. W.; Ayala, P. Y.; Morokuma, K.; Voth, G. A.; Salvador, P.; Dannenberg, J. J.; Zakrzewski, V. G.; Dapprich, S.; Daniels, A. D.; Strain, M. C.; Farkas, O.; Malick, D. K.; Rabuck, A. D.; Raghavachari, K.; Foresman, J. B.; Ortiz, J. V.; Cui, Q.; Baboul, A. G.; Clifford, S.; Cioslowski, J.; Stefanov, B. B.; Liu, G.; Liashenko, A.; Piskorz, P.; Komaromi, I.; Martin, R. L.; Fox, D. J.; Keith, T.; Al.Laham, M. A.; Peng, C. Y.; Nanayakkara, A.; Challacombe, M.; Gill, P. M. W.; Johnson, B.; Chen, W.; Wong, M. W.; Gonzalez, C.; Pople, J. A. *Gaussian 03, revision C.02*; Gaussian, Inc.: Wallingford, CT, 2004.
(54) (a) Klamt, A.; Schurmann, G. COSMO: a new approach to dielectric screening in solvents with explicit expressions for the screening energy and its gradient. *J. Chem. Soc., Perkin Trans. 2* **1993**, *2*, 799–805. (b) Barone, V.; Cossi, M. J. Quantum calculation of molecular energy gradients in solution by a conductor solvent model. *J. Phys. Chem. A* **1998**, *102*, 1995–2001.
(55) Miertus, S.; Scrocco, E.; Tomasi, J. Electrostatic interaction of a solute with a continuum. A direct utilization of ab initio molecular potentials for the prevision of solvent effects. *Chem. Phys.* **1981**, *55*, 117–129.
(56) Xiao, X.; Antony, S.; Pommier, Y.; Cushman, M. On the Binding of Indeno[1,2-*c*]isoquinolines in the DNA-Topoisomerase I Cleavage Complex. *J. Med. Chem.* **2005**, *48*, 3231–3238.
(57) Chen, A. Y.; Liu, L. F. DNA topoisomerases: essential enzymes and lethal targets. *Annu. Rev. Pharmacol. Toxicol.* **1994**, *34*, 191–218.
(58) Watt, P. M.; Hickson, I. D. Structure and function of type II topoisomerases. *Biochem. J.* **1994**, *303*, 681–695.
(59) Antony, S.; Agama, K. K.; Miao, Z.-H.; Hollingshead, M.; Holbeck, S. L.; Wright, M. H.; Varticovski, L.; Nagarajan, M.; Morrell, A.; Cushman, M.; Pommier, Y. Bisindenoisoquinoline bis-1,3-{(5,6-dihydro-5,11-diketo-11*H*-indeno[1,2-*c*]isoquinoline)-6-propylamino}propane bis(trifluoroacetate) (NSC 727357), a DNA intercalator and topoisomerase inhibitor with antitumor activity. *Mol. Pharmacol.* **2006**, *70*, 1109–1120.
(60) Harker, W. G.; Slade, D. L.; Drake, F. H.; Parr, R. L. Mitoxantrone resistance in HL-60 leukemia cells: reduced nuclear topoisomerase II catalytic activity and drug-induced DNA cleavage in association with reduced expression of the topoisomerase II β isoform. *Biochemistry* **1991**, *30*, 9953–9961.
(61) Denny, W. A.; Baguley, B. C. Dual topoisomerase I/II in Cancer Therapy. *Curr. Top. Med. Chem.* **2003**, *3*, 1349−1364, and references therein.
(62) Marmur, J.; Doty, P. Determination of the base composition of the deoxyribonucleic acid from its thermal denaturation temperature. *J. Mol. Biol.* **1962**, *5*, 109.
(63) Wada, A.; Kozawa, S. Instrument for the studies of differential flow dichroism of polymer solutions. *J. Polym. Sci., Part A: Polym. Chem.* **1964**, *2*, 853–864.
(64) (a) *MacroModel version 9.0*; Schrodinger Inc.: Portland, OR, 1998−2001.(b) Mohamadi, F.; Richards, N. G. J.; Guida, W. C.; Liskamp, R.; Lipton, M.; Caufield, C.; Chang, G.; Hendrickson, T.; Still, W. C. MacroModel−an integrated software system for modeling organic and bioorganic molecules using molecular mechanics. *J. Comput. Chem.* **1990**, *11*, 440–467.
(65) (a) Kaminski, G. A.; Friesner, R. A.; Tirado-Rives, J.; Jorgensen, W. J. Evaluation and reparametrization of the OPLS-AA force field for proteins via comparison with accurate quantum chemical calculations on peptides. *J. Phys. Chem. B* **2001**, *105*, 6474–6487. (b) Jorgensen, W. L.; Tirado-Rives, J. The OPLS Potential Functions for Proteins. Energy Minimization for Crystals of Cyclic Peptides and Crambin. *J. Am. Chem. Soc.* **1988**, *110*, 1657–1666.
(66) Pymol version 0.98. DeLano, W. L. *The PyMOL Molecular Graphics System*; DeLano-Scientific: San Carlos, CA, 2002; www.pymol.org.
(67) Allen, F. H.; Bellard, S.; Brice, M. D.; Cartwright, B. A.; Doubleday, A.; Higgs, H.; Hummelink, T.; Hummelink-Peters, B. G.; Kennard, O.; Motherwell, W. D. S. The Cambridge crystallographic data center: computer-based search, retrieval, analysis and display of information. *Acta Crystallogr., Sect. B: Struct. Sci.* **1979**, *35*, 2331–2339.
(68) (a) Huey, R.; Morris, G. M.; Olson, A. J.; Goodsell, D. S. A semiempirical free energy force field with charge-based desolvation. *J. Comput. Chem.* **2007**, *28*, 1145–1152. (b) Alonso, H.; Bliznyuk, A. A.; Gready, J. E. Combining docking and molecular dynamic simulations in drug design. *Med. Res. Rev.* **2006**, *26*, 531–568.

Downloaded by TATA INST OF FUNDAMENTAL RES on October 11, 2009 | http://pubs.acs.org
Publication Date (Web): August 19, 2009 | doi: 10.1021/jm900627v